

Dual broadband antenna with compact double ring radiators for IEEE 802.11 ac/b/g/n WLAN communication applications

Merih PALANDÖKEN*

Department of Electrical and Electronics Engineering, Faculty of Engineering and Architecture,
İzmir Kâtip Çelebi University, İzmir, Turkey

Received: 13.07.2015

Accepted/Published Online: 30.04.2016

Final Version: 10.04.2017

Abstract: In this paper, a dual broadband antenna is proposed for WLAN communication modules supported by the IEEE 802.11 ac/b/g/n standard. The antenna design is based on two interspaced electrically small split-ring resonators, each of which is directly fed through the stepped impedance microstrip line with an optimized electromagnetic coupling distance in between. The proposed dual band antenna operates in the lower frequency band from 2.3 GHz up to 3 GHz with 2.65 GHz center frequency (26.4 % bandwidth) and in the higher frequency band from 4.7 GHz up to 6 GHz with 5.35 GHz center frequency (24.3% bandwidth). The radiating section of the antenna is $\lambda_0/5.8 \times \lambda_0/10.2$ at 2.4 GHz in the lower WLAN frequency band. The return loss is numerically calculated and experimentally measured with the result of good agreement between them. The antenna gain values are 4.77 dBi, 2.9 dBi, and 2.45 dBi at 2.45 GHz, 5.2 GHz, and 5.8 GHz, respectively, with omnidirectional radiation patterns at the horizontal plane. The omnidirectional radiation patterns at both frequency bands allow the proposed WLAN antenna to be utilized for modern mobile broadband wireless network applications.

Key words: Wireless communication, ring resonators, dual broadband microstrip antennas

1. Introduction

Wireless local area networks (WLANs) are quite important wireless infrastructures in the context of allowing location-independent network access for wireless computing devices such as sensor and computer networks with high speed connectivity. They are also standardized depending on the wireless access range, data rate, and power consumption levels, such as in the form of IEEE 802.11. The increasing demand rate of WLANs to be utilized in daily life has resulted in different antenna structures to be designed with low profiles, light weights, flush mounting, and single feeds to fit the limited equipment space of WLAN devices. Many antenna types designed to meet WLAN standard requirements have been developed and presented [1–15]. These antennas are designed in the form of zigzag-shaped rectangular patch radiators [1], L- and U-shaped slot loaded monopole radiators [2,3], L-shaped slot fed parasitic patch radiators [4], fork-shaped monopole radiators [5,6], E-shaped monopole radiators [7], and circular ring radiators with Y-shaped feeding lines [8]. In addition, there are alternative antenna designs, which are inspired by the metamaterial unit cell geometries utilized in artificial material design [9–18]. They are designed in the form of metamaterial reactive loaded antennas with inverted L-shaped slot defected ground planes [9], triangular-shaped split-ring resonator (SRR) terminated slot radiators [10], complementary SRR loaded monopole antennas [11,12], open-ended ring antennas with discrete chip

*Correspondence: merih.palandoken@ikc.edu.tr

inductors [13], inductively coupled two open-ended loop radiators [14], and meandering SRR slot loaded Y-shaped monopole radiators [15]. Among the well-known microstrip antennas, these planar monopole antennas have received much more interest than other antenna types due to their potentials resulting in required radiation features of dual band or multiband, wide bandwidth, and low profile for a wireless communication system [1–18].

In this paper, a broadband WLAN antenna with a compact radiator composed of two interspaced ring resonators is proposed for dual band operation in the IEEE 802.11 ac/b/g/n standards. The SRRs are directly connected to the microstrip line on a truncated ground plane with a certain phase shift in between for dual broadband operation. The effect of coupled resonances between the larger and smaller ring resonators with different magnetic coupling mechanisms at lower and higher frequencies makes the antenna operate in a broadband manner in two frequency bands. This form of coupling mechanism through the feeding line to control the lower and upper frequency bands in a broadband manner is the novelty of the current design in comparison to the alternative designs with similar resonator geometries [9–15]. The ground plane is structured in the form of a truncated ground plane to enhance the radiation performance in addition to an omnidirectional radiation pattern necessary for wireless communication networks. The antenna is matched to 50Ω line impedance with the stepped impedance transformer at WLAN bands of 2.4 GHz and 5.2–5.8 GHz in IEEE 802.11 b/g/n and IEEE 802.11 ac, respectively. The antenna geometry and design principle are explained in Section 2. The numerical computation and measurement results of return loss, radiation pattern, and gain at both frequency bands are presented in Section 3 in addition to the resonant current distributions. The concluding remarks are given in Section 4.

2. Antenna configuration and design consideration

The antenna geometry is shown in Figure 1 along with the enlarged compact radiator and fabricated prototype. The proposed antenna utilizes the main principle of capacitive and inductive coupling of two open-ended ring resonators with different resonance frequencies and the resulting band broadening effect of capacitive and inductive resonator loading. These two resonators are directly connected to the transmission line to increase the coupling effect between them. The separation distance is optimized to increase the coupling of both resonators with the connecting transmission line section. The physical dimensions of the antenna are listed in Table 1. Both resonators, which are coupled galvanically to the feeding line, are used as the radiating elements in conjunction with a narrow band electrically small feeding monopole line. The side lengths of larger and smaller resonators are determined to excite $\lambda/2$ resonance modes in the lower and higher frequency bands, respectively. These electrically small resonators are the fundamental unit cell structures in the design of artificial magnetic materials with resonant magnetic permeability [18]. The antenna is matched to 50Ω line impedance with the stepped impedance transformer for broadband WLAN operation. The feeding line is in the form of a microstrip line to excite the desired resonance modes of two mainly magnetically coupled resonators for the dual band operation. The ground plane is truncated to an optimum length to result in the desired mode radiation in both directions with high gain in the dual band due to the lack of reflecting ground underneath. The ground plane is large in size in order for the antenna to be utilized without need of in-system integration. It is not necessary to use ferrite chokes to isolate the feeding cable from the antenna near field, which improves the electromagnetic compatibility of the antenna.

The feeding line width is 3 mm for 50Ω line impedance. The substrate is 6 cm \times 9 cm \times 1.6 mm double-sided low-cost FR4-epoxy material with the metal thickness of 0.018 mm, relative permittivity of 4.4, and loss tangent of 0.02.

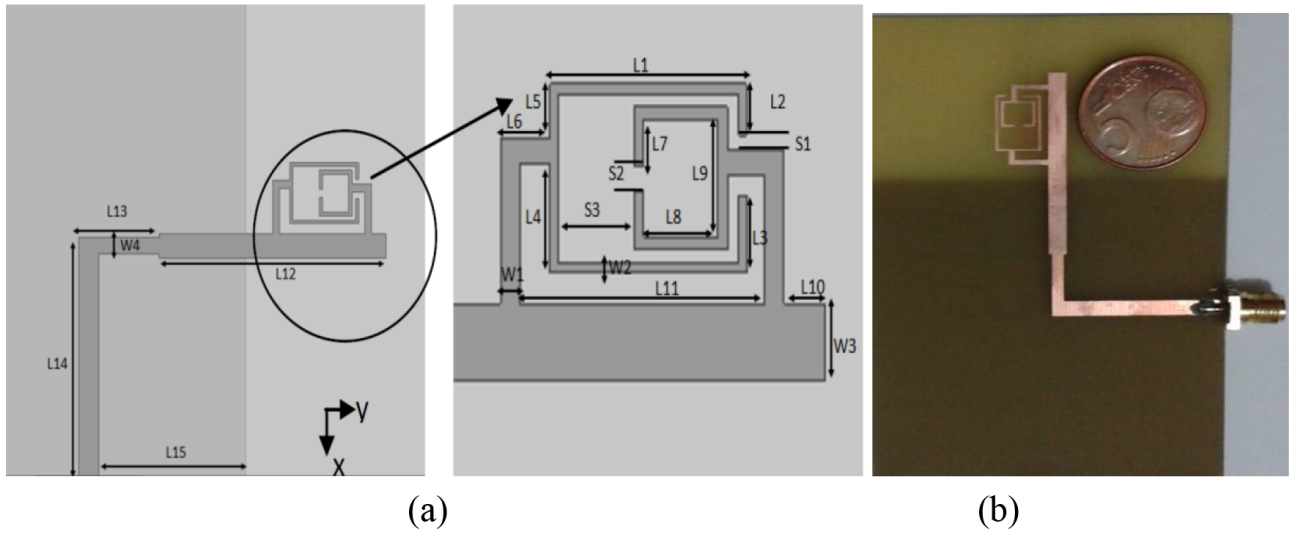


Figure 1. a) Antenna model with geometrical parameters, b) antenna prototype.

Table 1. WLAN antenna geometrical parameters (mm).

L1	10.25	L2 = W4	2	L3	3
L4	4.3	L5	2.1	L6	2.6
L7	2.35	L8	3.85	L9	4.6
L10	2.2	L11	12.8	L12	34
L13	12	L14	29	L15	22
W1	2.6	W2	0.4	W3	3
S1	0.6	S2	1	S3	4

3. Numerical and experimental results

The electromagnetic response of the broadband microstrip WLAN antenna is numerically calculated in a 3D full-wave FEM-based electromagnetic field solver, ANSYS HFSS, to investigate the reflection parameter and radiation performance. The fabricated antenna prototype is measured with an Anritsu MS2721B spectrum analyzer in connection with a KDC-2/8-10S 2–8 GHz broadband directional coupler. The simulation and measurement results of reflection parameter are shown in Figure 2.

The lower frequency band extends from 2.18 GHz up to 2.76 GHz for the simulated S11 and from 2.3 GHz up to 3 GHz for the measured S11, whereas the higher frequency band extends from 4.8 GHz up to 6.1 GHz for the simulated S11 and from 4.7 GHz up to 6 GHz for the measured S11. The measurement and simulation results have good agreement. There are low frequency ripples superimposed on the measurement results. The first reason for this unwanted phenomenon is the multiple resonance effect resulting from the feeding cable as a calibration error. The second reason is the impedance mismatch between the feeding coaxial cable and microstrip line due to the geometrical modifications of the fabricated prototype with respect to the design parameters. The simulated resonance frequencies are shifted to the higher frequencies in the measurement result due to the permittivity uncertainty of substrate material in addition to the geometrical changes in the prototype. The surface current distributions at the resonance frequencies of the two bands are shown in Figures 3a and 3b to help understand the operation principle of the antenna. The surface current distribution at 2.45 GHz is due to

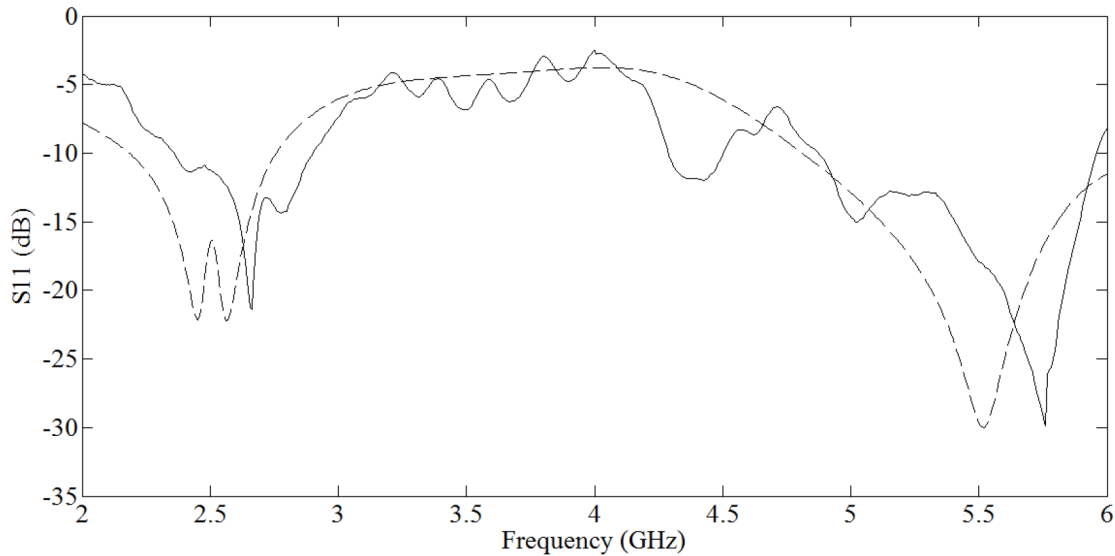


Figure 2. Measured (solid) and simulated (dashed) S11 of dual broadband WLAN antenna.

the resonance excitation of the larger ring resonator with the magnetic coupling to the smaller ring resonator. The mutual magnetic coupling between the two resonators is positive, which is one reason why the resonance frequency at the lower frequency band is split into two resonance frequencies. However, the surface current distribution at 5.5 GHz results from the resonance excitation of the smaller ring resonator with the negative mutual magnetic coupling to the larger ring resonator. The mutual coupling between two resonators leads the higher frequency band to be broadened. However, as shown in Figure 3b, the surface current distributions of the inner and outer resonators at 5.5 GHz result in oppositely directed resonant magnetic dipoles, which reduces the radiation efficiency and gain in the higher frequency band. As shown in Figure 3a, this is not the case for the lower frequency band, which results in higher gain values due to the resonant magnetic dipoles being directed in the same direction. Various numerical calculations for the geometric parameters of the impedance matching line, ground plane, and resonator size have been performed to excite two resonance modes in a broadband manner. The lengths of the stepped impedance transmission line and inner/outer resonator sizes are optimized to control the resonance frequencies and respective bandwidths of the lower and higher frequency bands. Because of the large electrical length of the stepped impedance transformer, the effect of the ground plane size is significant for the optimum antenna operation, as shown in Figure 4. The antenna gains are enhanced respectively depending on how well the antenna input impedance is matched for the optimum geometric parameters. The proposed antenna design is compared to the alternative WLAN designs with similar resonator geometry in Table 2. As shown in Table 2, the proposed antenna has high and acceptable gain values in the lower and higher frequency bands in a broadband manner with compact radiator size.

The normalized radiation patterns of the dual broadband WLAN antenna at three frequencies on the horizontal (XY) and vertical (YZ) planes for co- and cross-polarizations are shown in Figure 5. The antenna gain values for both frequency bands are also plotted in Figure 6. As shown in Figure 6, the gain is larger than 3.3 dBi in the lower frequency band with a maximum gain of 5.24 dBi at 2.2 GHz. The gain at the lower WLAN frequency, 2.4 GHz, is 4.76 dBi. The gain in the higher frequency band is lower than that in the lower frequency band. The reason for this is the oppositely directed magnetic dipoles in the inner and outer resonators, which reduces the radiation efficiency and gain. However, the gain values are at an acceptable level with 2.9 dBi and

2.44 dBi at 5.2 GHz and 5.8 GHz WLAN frequencies in the higher frequency band, respectively. The antenna has almost omnidirectional radiation patterns for both polarizations, which makes the antenna positioning more flexible due to a permissible signal receiving level at both polarizations.

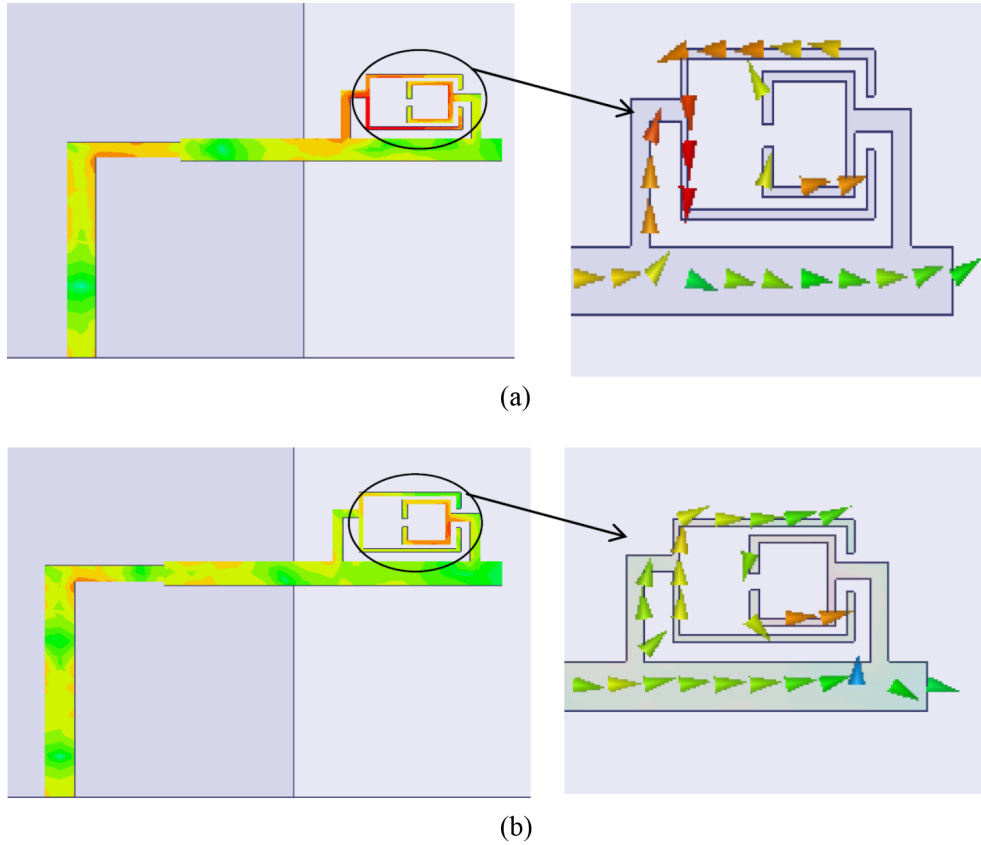


Figure 3. Surface current distributions of WLAN antenna at (a) 2.45 GHz and (b) 5.5 GHz.

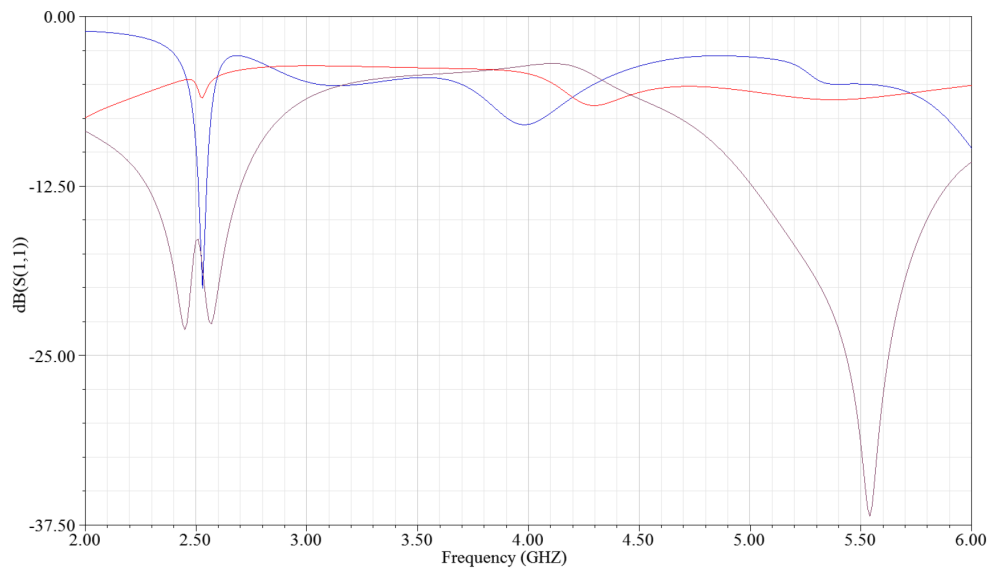


Figure 4. The effect of ground plane size on S11 for $L_{15} = 12$ mm (red), 22 mm (brown), and 32 mm (blue).

Table 2. Comparison of alternative WLAN antennas.

Reference	Gain	BW	Radiator size at 2.4 GHz
[9]	1.14 dBi (2.45 GHz) 1.78 dBi (5.5 GHz)	3.28% (2.4–2.48 GHz) > 40% (5.2 GHz to beyond 7 GHz)	$\lambda_0/6.25 \times$ $\lambda_0/5.31$
[10]	2.63–3.22 dBi (2 GHz band) 2.5–3.07 dBi (5 GHz band)	75.47% (1.96–4.33 GHz) 35.50% (5.05–7.23 GHz)	$\lambda_0/4.16 \times$ $\lambda_0/6.25$
[11]	-1 dBi (2 GHz band) 4 dBi (5 GHz band)	17% (2.4–2.84 GHz) 3.8% (5.15–5.35GHz)	$\lambda_0/4.8 \times$ $\lambda_0/9$
[12]	0.94 dBi (2.5 GHz) 2.61 dBi (5.5 GHz)	13.43% (2.36–2.7 GHz) 19.96% (5.01–6.12 GHz)	$\lambda_0/4.46 \times$ $\lambda_0/10.41$
This work	4.76 dBi (2.4 GHz) 2.9 dBi (5.2 GHz) 2.44 dBi (5.8 GHz)	26.4% (2.3–3 GHz) 24.3% (4.7–6 GHz)	$\lambda_0/5.8 \times$ $\lambda_0/10.2$

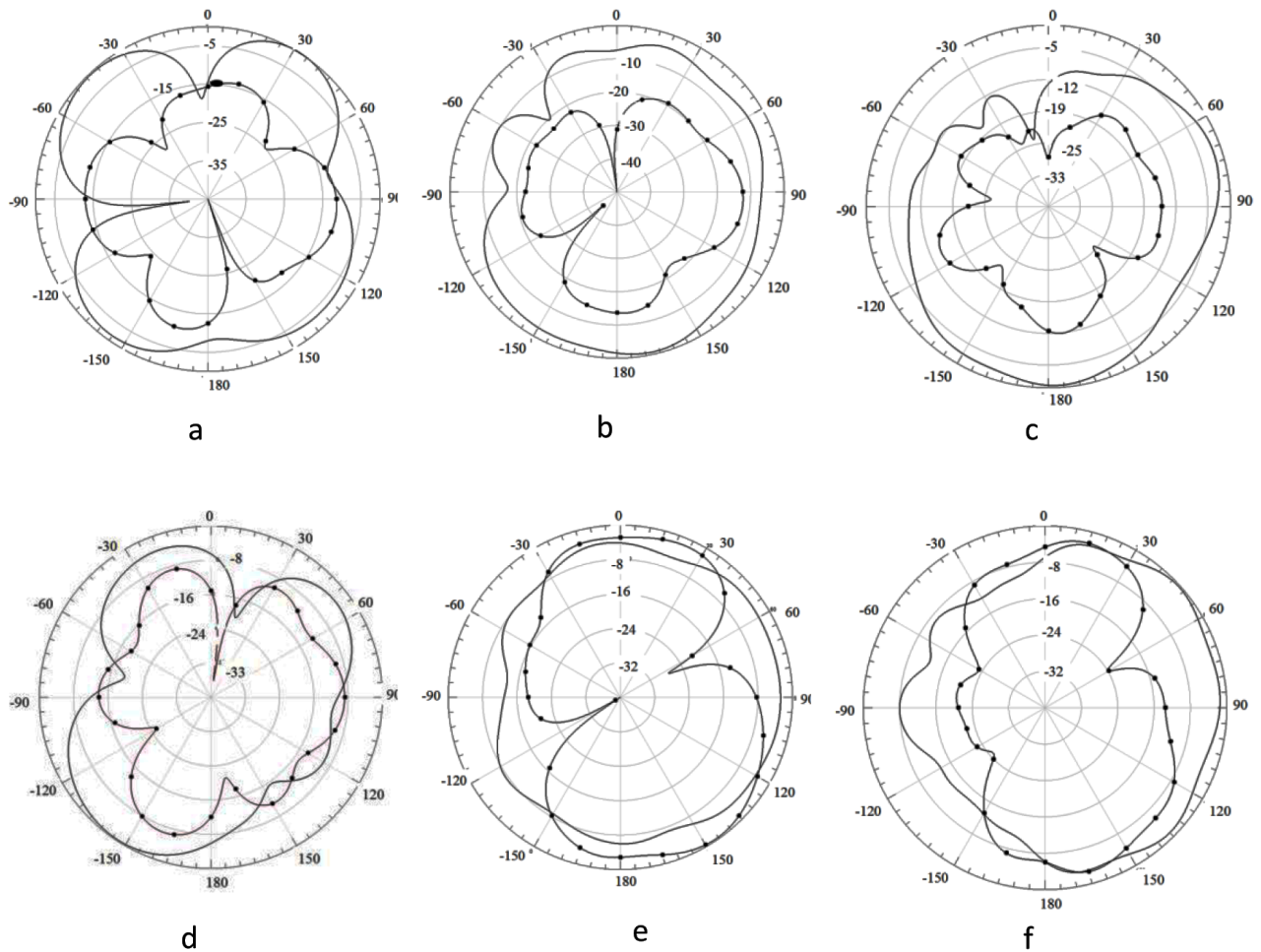


Figure 5. Normalized radiation patterns for copolarization (solid) and cross-polarization (filled circle) at horizontal (XY) plane for (a) 2.4 GHz, (b) 5.2 GHz and (c) 5.8 GHz and at vertical (YZ) plane for (d) 2.4 GHz, (e) 5.2 GHz, and (f) 5.8 GHz.

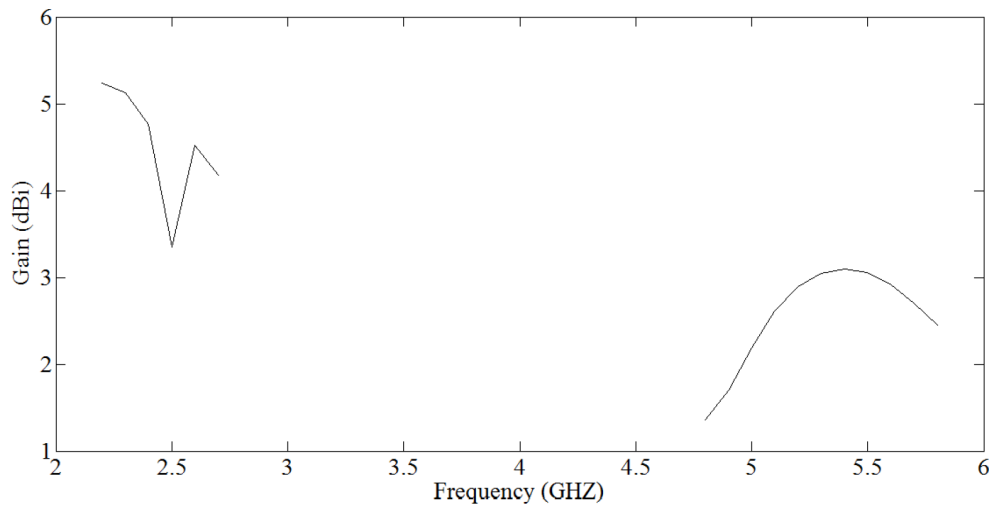


Figure 6. Gain (dBi) of dual broadband WLAN antenna at two frequency bands.

4. Conclusion

In this paper, a dual broadband WLAN antenna with compact radiator, composed of two interspaced ring resonators, is numerically and experimentally studied. The intercoupling mechanism between the inner and outer resonators in the form of direct connection with the feeding line is a novelty to control the impedance bandwidth at WLAN frequencies. The proposed antenna is compared to the alternative WLAN antenna designs, which indicates better impedance bandwidth and radiation performance in compact radiator size. The return loss is numerically calculated and measured. The measurement and simulation results agree well. The WLAN antenna has impedance bandwidth of 700 MHz between 2.3 GHz and 3 GHz in the lower band and of 1.3 GHz between 4.7 GHz and 6 GHz in the higher frequency band. The antenna gains are 4.76 dBi, 2.9 dBi, and 2.44 dBi at 2.4 GHz, 2.5 GHz, and 2.6 GHz, respectively. The omnidirectional radiation patterns in dual broad frequency bands with permissible gain values allow the proposed antenna to be utilized in wireless communication modules supported by the IEEE 802.11 ac/b/g/n standard.

References

- [1] Pakkathillam JK, Kanagasabai M. Performance evaluation of a dual band paper substrate wireless sensor networks antenna over curvilinear surfaces. *IET Microw Antenna P* 2015; 9: 715-722.
- [2] Moosazadeh M, Kharkovsky S. Compact and small planar monopole antenna with symmetrical L- and U-shaped slots for WLAN/WiMAX applications. *IEEE Antenn Wirel Pr* 2014; 13: 388-391.
- [3] Chen H, Yang X, Yin YZ, Fan ST, Wu JJ. Triband planar monopole antenna with compact radiator for WLAN/WiMAX applications. *IEEE Antenn Wirel Pr* 2013; 12: 1440-1443.
- [4] Huang H, Liu Y, Zhang S, Gong S. Multiband metamaterial-loaded monopole antenna for WLAN/WiMAX applications. *IEEE Antenn Wirel Pr* 2015; 14: 662-665.
- [5] Luo Q, Pereira JR, Salgado HM. Compact printed monopole antenna with chip inductor for WLAN. *IEEE Antenn Wirel Pr* 2011; 10: 880-883.
- [6] Yoon JH, Rlee YC. Design of a microstrip-fed monopole antenna with a rectangular slit ground and a rectangular projection strip for dual-band WLAN operations. *Microw Opt Techn Let* 2012; 54.4: 1039-1044.
- [7] Mehdipour A, Sebak, AR, Trueman CW, Denidni, TA. Compact multiband planar antenna for 2.4/3.5/5.2/5.8-GHz wireless applications. *IEEE Antenn Wirel Pr* 2012; 11: 144-147.

- [8] Pei J, Wang AG, Gao S, Leng W. Miniaturized triple-band antenna with a defected ground plane for WLAN/WiMAX applications. *IEEE Antenn Wirel Pr* 2011; 10: 298-301.
- [9] Zhu J, Antoniadis MA, Eleftheriades GV. A compact tri-band monopole antenna with single-cell metamaterial loading. *IEEE T Antenn Propag* 2010; 58: 1031-1038.
- [10] Yang K, Wang H, Lei Z, Xie Y, Lai H. CPW-fed slot antenna with triangular SRR terminated feedline for WLAN/WiMAX applications. *Electron Lett* 2011; 47: 685-686.
- [11] Basaran SC, Olgun U, Sertel K. Multiband monopole antenna with complementary split-ring resonators for WLAN and WiMAX applications. *Electron Lett* 2013; 49: 636-638.
- [12] Kang L, Wang H, Wang XH, Shi X. Compact ACS-fed monopole antenna with rectangular SRRs for tri-band operation. *Electron Lett* 2014; 50: 1112-1114.
- [13] Kim WS, Choi S, Jeong GT. A low-profile WLAN antenna with inductor and tuning stub for broadband impedance matching. *International Journal of Antennas and Propagation* 2014; 2014: 452160.
- [14] Zhou X, Quan XL, Li RL. A dual-broadband MIMO antenna system for GSM/UMTS/LTE and WLAN handsets. *IEEE Antenn Wirel Pr* 2012; 11: 551-554.
- [15] Liu P, Zou Y, Xie B, Liu X, Sun B. Compact CPW-fed tri-band printed antenna with meandering split-ring slot for WLAN/WiMAX applications. *IEEE Antenn Wirel Pr* 2012; 11: 1242-1244.
- [16] Palandoken M, Grede A, Henke H. Broadband microstrip antenna with left-handed metamaterials. *IEEE T Antenn Propag* 2009; 57: 331-338.
- [17] Palandöken M. Artificial materials based microstrip antenna design. In: Nasimuddin N, editor. *Microstrip Antennas*. Rijeka, Croatia: InTech, 2011. pp. 43-68.
- [18] Caloz C, Itoh T. *Electromagnetic Metamaterials: Transmission Line Theory and Microwave Applications*. 1st ed. Hoboken, NJ, USA: Wiley, 2005.